Chemical and optical phototransformation of dissolved organic matter

Chemical and optical phototransformation of dissolved organic matter

Steven Loiselle,[a,b*] Davide Vione,[c,d] Claudio Minero,[c] Valter Maurino,[c] Antonio Tognazzi, [a,b] Arduino M. Dattilo, [a,b] Claudio Rossi, [a,b] Luca Bracchini [a,b]

[a] *Dip. Farmaco Chimico Tecnologico, Università degli Studi di Siena, Via Aldo Moro 2, 53100 Siena, Italy.*

[b] *CSGI (Inter-University Center for Colloid and Surface Science), Via della Lastruccia 3, 50019 Sesto Fiorentino (FI), Italy.*

[c] *Dipartimento di Chimica Analitica, Università degli Studi di Torino, Via Pietro Giuria 5, 10125 Torino, Italy. http://www.environmentalchemistry.unito.it.*

[d] *Centro Interdipartimentale NatRisk, Università degli Studi di Torino, Via Leonardo da Vinci 44, 10095 Grugliasco (TO), Italy. http://www.natrisk.org.*

loiselle@unisi.it, tel +39 0577 234360, fax +39 0577 234 177, Università degli Studi di Siena, Via Aldo Moro 2, 53100 Siena, Italy.

Abstract

Dissolved organic matter represents the main reservoir of organic carbon in most aquatic ecosystems. In the present study, we determined the optical changes and the quantum yields of transient species formation for chromophoric dissolved organic matter (CDOM) samples undergoing photodegradation. The results show that the triplet states ^{3}CDOM* are potentially key players in CDOM photodegradation and that such transformations are strongly influenced by small differences in CDOM sources and sinks. In contrast, $^{\bullet}$OH radicals are very unlikely to play a key role in phototransformation. These results represent an important first step in combining optical and transient species analyses to understand photodegradation processes of dissolved organic matter.

Keywords: photochemistry; photogenerated transients; direct and sensitized photolysis; absorption spectral slope; photobleaching.

1. Introduction

Dissolved organic matter (DOM) is a complex mixture of organic compounds with spatial and temporal distributions that result from multiple sources and sinks (Tranvik et al., 2009; Bracchini et al., 2011). DOM sources in most ecosystems can be distinguished as autochthonous (produced *in situ* by biological activity from aquatic macrophytes, phytoplankton, zooplankton, bacterioplankton, ...) or allochthonous (of terrestrial origin, usually originating from the degradation of terrestrial organic matter). These two DOM pools differ in their optical and chemical characteristics (Sulzberger and Durisch-Kaiser, 2009; Zhang et al. 2009). Dominant sinks of DOM include direct photodegradation, reaction with photogenerated transient species, biological degradation and flocculation (Moran et al., 2000; Chen et al., 2007). The importance of each sink will depend on the local conditions as well as the chemical and optical characteristics of the DOM present.

Solar ultraviolet radiation can directly modify properties of the chromophoric fraction of dissolved organic matter (CDOM) through photolysis. However, indirect phototransformation may also play an important role in altering CDOM composition (Vione et al., 2009a, 2010a). The term indirect photodegradation has been used with two different meanings in the scientific literature. One concerns the loss in absorption at wavelengths that are not present in the incident irradiance (Del Vecchio and Blough, 2004). The other is linked to the formation and subsequent reactivity of transient species such as hydroxyl radicals ($^{\bullet}OH$), singlet oxygen ($^1O_2$) and triplet excited states of dissolved organic matter (^{3}CDOM*) that are generated during irradiation of CDOM (Boreen et al., 2008). The fact that some or most of the reactive species that could be involved in the transformation of DOM/CDOM are photochemically generated by CDOM itself, suggests that CDOM is at the same time a producer and a scavenger of reactive phototransients (Hoigné, 1990; Canonica and Freiburghaus, 2001; Al Housari et al., 2010; Minella et al., 2011). Few attempts have been made so far to associate the production of transient species with optical changes in CDOM.

In the present study, we compared changes in CDOM optical properties to the production of transient species in controlled photodegradation experiments. Rates of transient formation and rates of photodegradation were compared to identify the transient species that dominate CDOM dynamics in a small coastal lake.

2. Experimental section

2.1. Sampling

Sampling and measurements were made in Fogliano Lake in May 2009 (Figure 1). The lake is a small coastal lake (4 km^2) in the National Park of Circeo in central Italy. Two sampling sites (F1 and F2) were chosen to examine the CDOM variability due to small differences in sources and sinks. The F1 site was located in the centre of the lake, 200 m from the tidal sea gate that connects the lake to the Tyrrhenian Sea. The F2 site was located in the northeast part of the lake which is bordered by agriculture areas but has no direct surface freshwater inputs. The average depth of the lake is around 1 m and the lake bottom is characterized by extensive areas of submerged macrophytes (*Ruppia maritima* and *Zoostera noltii*), particularly evident in the northeast part of the lake during the summer (Signorini et al., 2008). The spatial distribution of vertical light attenuation shows that the water of the F2 area has a higher UV attenuation (Bracchini et al., 2005). Hydrodynamic models also indicate that the water residence time is higher in this part of the lake (Bartocci et al. personal comm.).

Temperature, pH, specific conductance and dissolved oxygen profiles were performed at each sampling site using a Hydrolab Datasonde 3 (Hydrolab Corp., USA), calibrated prior to each measurement. Chlorophyll-*a* fluorescence and nephelometric turbidity were estimated using daily averages obtained from a portable fluorometer (SCUFA Submersible Fluorometer, Turner Designs, excitation wavelength = 485 nm, emission wavelength = 680 nm). The fluorometer response was calibrated daily using a standard solution and measurements of chlorophyll-*a* concentrations [*sensu* Talling and Driver (1963)] from different lakes including Fogliano Lake. Despite the different sources of variability in the chlorophyll-*a* fluorescence (*e.g.*, quenching, temperature, package effect and self-shading), the measured concentrations and fluorescence signals showed a good linear regression (R^2 = 0.74, $p < 0.001$). Nephelometric turbidity calibration used a standard formazine suspension.

2.2. CDOM Absorption measurements

Lake samples (1 liter) were obtained nearly simultaneously from two sampling sites (F1, F2) at a depth of 0.5 m. Samples were filtered in series using sterile filter membranes, with a porosity of 0.8 μm and 0.22 μm (cellulose acetate membranes, Sartorius, Minisart), under low N_2 pressure. Filters

were initially pre-conditioned by using 200 mL of the sample. Filtered samples, sealed with Teflon caps were stored in amber glass bottles at 4°C in the absence of light until analysis. Spectrophotometric analysis (Perkin Elmer Lambda 25, Varian Cary 100) was performed using a single 0.01 m quartz cuvette. Samples were acclimatized to room temperature (18 °C) and absorbance spectra (A) were recorded from 240 nm to 700 nm with a spectral resolution of 1 nm (measured absorbance range 0.0800 - 0.0009 AU). Milli-Q water (at the same temperature of the samples) was used as a reference. Three complete scans (1920 nm min^{-1}) of each sample were performed and the average values were calculated. The differences between the scans were close to the detection limit of the spectrophotometer ($4 \cdot 10^{-4}$ AU). The average absorbance value between 680-700 nm was used as a null point adjustment for the absorption spectra. Absorbance data were converted into absorption coefficients using $a_\lambda = 2.303 A_\lambda \bullet / L$, where L is the cuvette pathlength (0.01 m).

A distribution of absorption spectral slopes was estimated using 20 nm wavelength intervals and a 1 nm step from 240 nm to 680 nm. For each 20 nm wavelength interval, an estimate of spectral slope, fitting value (R^2) of the exponential fitting and residuals were determined using a nonlinear regression fitting method (Loiselle et al., 2009a). The minimization of the least squares between residuals and the experimental data was based on the Levenberg-Marquardt algorithm. The resultant distribution of spectral slopes ($S(\lambda)$, nm^{-1}) was plotted as a function of wavelength. The exponential fitting values were used to identify wavelength intervals where the assumption of exponential behavior was significant ($R^2 > 0.95$, $p < 0.001$).

2.3. Determination of nitrate, nitrite and Non-Purgeable Organic Carbon (NPOC) in lake water

The concentration of nitrate in lake water was determined with a Dionex DX 500 Ion Chromatograph, equipped with Rheodyne injector (20 µL sample loop), LC 30 chromatography oven, GP 40 gradient pump, Dionex Ion Pac AG9-HC 4-mm (10-32) guard column, Dionex Ion Pac AS9-HC 4-mm (10-32) anion exchange column, ASRS-ULTRA 4-mm conductivity suppression unit, and ED 40 electrochemical detector, operated in conductivity mode at 30°C. The eluent was a $1.1 \cdot 10^{-2}$ M K_2CO_3 / $4.5 \cdot 10^{-3}$ M $NaHCO_3$ mixture, flow rate was 1.00 mL min^{-1}, and the retention time of nitrate was 6.75 min (column dead time 2.60 min).

Nitrite was quantified following the procedure of Kieber and Seaton (1996) using High Performance Liquid Chromatography coupled with UV-vis detection.

Non-Purgeable Organic Carbon (NPOC) was determined with a Shimadzu TOC-V_{CSH} Total Organic Carbon Analyzer, equipped with an ASI-V autosampler and fed with zero-grade air. Each lake water sample was acidified with 2 M HCl (1.5% v/v) and sparged for 10 min with zero-grade air prior to injection and catalytic combustion of organic compounds into CO_2.

2.4. Irradiation experiments.

Two different series of phototransformation experiments were performed on each filtered lake water sample. One series examined photo-induced formation of reactive transient species in controlled laboratory conditions. The other series used solar radiation over several days in monitored lake conditions to determine the direct and indirect modification of the optical characteristics of the lake CDOM.

In the transient species experiments, irradiance was provided by a set of five UVA lamps (TL K05, Philips) with a constant spectral irradiance on cylindrical Pyrex cells over a 30 hour period. The cells (4.0 cm diameter, 2.5 cm height, with a lateral neck and screw cap) were filled with 20 mL of filtered lake sample, leaving about 10 mL headspace, and were magnetically stirred during irradiation. The incident UV irradiance (290 - 400 nm) was 57 W m^{-2}, measured with a CO.FO.ME.GRA. power meter (Milan, Italy). The emission spectra were determined using an Ocean Optics SD2000 CCD spectrophotometer (Figure 2a). The photon flux in solution ($1.1 \cdot 10^{-5}$ Einstein L^{-1} s^{-1}) was actinometrically determined using ferrioxalate, considering the spectral trends of ferrioxalate absorption and of the quantum yield of Fe^{2+} photoproduction (Kuhn et al., 2004). The emission spectrum of the lamps was normalized to the actinometry data and the transmittance of Pyrex (Albinet et al., 2010). The cell pathlength was 0.016 m.

In the *in-situ* photodegradation experiments, exposure of filtered lake samples to incident solar radiation was performed in 1 L sterile Tedlar (polyvinylfluoride) sampling bags, after assuring that the bags did not contribute to CDOM absorption or sample bias (Loiselle et al., 2009b). A set of control samples was created by covering additional bags with dark adhesive tape. Sample and control bags containing filtered lake samples were then fixed in a horizontal position on the lake, just below the surface of the water (< 1 cm depth). Surface irradiance measurements were obtained every minute directly above the lake (1 m) using cosine corrected multichannel (SKR 1850) and single channel sensors (SKR 420, 430) for ultraviolet A (UVA, 315-380 nm) and ultraviolet B (UVB, 280-315 nm) (Skye Instruments LTD, UK). The sensor calibration was performed in March

2009 using a StellarNet deuterium lamp (model #SL3). The spectral incident irradiance ($E_o(\lambda, t)$, kW m^{-2} nm^{-1}) was calculated by considering the total solar irradiance on the sample bag and the spectral transmission of the Tedlar bags from 280 to 400 nm (Figure 2b).

The cumulative UV irradiance dose (D) was determined in both experiments considering the initial absorption spectrum for each sample together with the incident irradiance within the sample container (cell, bag) as $D = \int_{280}^{400}\int_{0}^{t}\left(E_o(\lambda,t) - E_x(\lambda,t)\right)dt\,d\lambda = \int_{280}^{400}\int_{0}^{t} E_o(\lambda,t)(1-e^{-a(\lambda)x})\,dt\,d\lambda$, where x is the optical pathlength of the sample, $E_o(\lambda,t)$ is the incident irradiance, a is the sample spectral absorption for each wavelength and t is the irradiation time (Table 2). Loss due to scattering in the filtered samples was assumed to be not significant with respect to absorption.

Photodegradation rates were determined by using the derivative of the change in absorption and S(λ) with increasing dose. Over the limited duration of the present experiment, the assumption of a linear decrease was suitable for data fit. However, for long term photodegradation experiments, the change in absorption (or spectral slope) will not be linear, hence the derivative of the change in absorption (or S(λ)) with dose will not be constant over time.

2.5. Measurement of rates of reactive species photoproduction.

The transformation reaction of benzene into phenol was used as a probe for $^{\bullet}OH$, the transformation of 2,4,6-trimethylphenol was used for ^{3}CDOM*, and the transformation of furfuryl alcohol was used for $^1O_2$ (Al Housari et al., 2010). Filtered lake water samples (20 mL) were spiked with benzene (initial concentration of 3.0 mM), furfuryl alcohol (FFA, 1.8 mM) or 2,4,6-trimethylphenol (TMP, 2.0 mM) and placed into Pyrex glass cells, tightly closed with a lateral screw cap. After irradiation (up to 30 h), the cells were refrigerated in the dark for 15 min to avoid the loss of volatile compounds (*e.g.* benzene). The aqueous solutions were analyzed by HPLC-UV with a RP-C18 column. HPLC conditions for the different compounds are reported in Vione et al. (2010) and Minella et al. (2011). Formation of phenol and degradation of FFA or TMP were negligible for samples when irradiated in ultra-pure water and for lake samples stored in the dark.

The time evolution data of phenol from benzene in irradiated lake water were fitted using the equation

$$P_t = k_f^P\ B_o\ (k_d^P - k_d^B)^{-1}\ [\exp(-k_d^B t) - \exp(-k_d^P t)] \qquad (1)$$

where P_t is the concentration of phenol at the time t, B_o the initial benzene concentration, k_f^P and k_d^P the pseudo-first order rate constants for the formation and the transformation of phenol, respectively, and k_d^B the pseudo-first order rate constant for the transformation of benzene. The initial formation rate of phenol is $R_P = k_f^P B_o$. Phenol formation is accounted for by reaction between benzene and $^\bullet$OH (Takeda et al., 2004), phenol transformation by reaction with $^\bullet$OH and/or ^{3}CDOM* (Canonica and Freiburghaus, 2001). The ^{3}CDOM* reaction is expected to prevail, because it plays the main role also under conditions where degradation by $^\bullet$OH is strongly favored (Vione et al., 2009c).

The time evolution data of TMP and FFA were fitted by $C^i_t = C^i_o \exp(-k_d^i t)$, where C^i_t is the concentration of the substrate i (i = FFA or TMP) at the time t, C^i_o the initial concentration of i, and k_d^i the pseudo-first order transformation rate constant of i. The initial transformation rate of the substrate i is given by $R_i = k_d^i C^i_o$. The errors associated to the rates were derived at the σ level from the scattering of the experimental data (obtained as the average of replicate runs) around the fit curves.

The reaction between benzene and $^\bullet$OH produces phenol with a yield of 95% (Takeda et al., 2004). This reaction competes with the scavenging of the hydroxyl radicals by the natural scavengers present in lake water. Therefore, the initial formation rate of phenol is expressed by the following equation:

$$R_P = 0.95\, R_{OH} \frac{k_{B,OH}\, B_o}{k_{B,^\bullet OH}\, B_o + \sum_i k_{S_i}\, S_i} \qquad (2)$$

where R_{OH} is the formation rate of $^\bullet$OH, $k_{B,OH} = 7.8\times10^{-9}$ M^{-1} s^{-1} is the second-order rate constant for the reaction between benzene and $^\bullet$OH (Buxton et al., 1988), B_o = 3 mM, and $\Sigma_i\, k_{Si}\, S_i$ is the rate constant for the scavenging of $^\bullet$OH by the natural components of the water sample (Takeda et al., 2004). For most surface waters the value of $\Sigma_i\, k_{Si}\, S_i$ varies between 10^4 and 5×10^5 s^{-1} (Vione et al., 2010a, and references therein). In the presence of 3.0 mM benzene, $k_{B,OH}\, B_o = 2.3\times10^7$ s^{-1}, which allows the natural scavenging rate constant $\Sigma_i\, k_{Si}\, S_i$ to be neglected in equation (2). With this approximation one gets $R_P = 0.95\, R_{OH}$ and, as a consequence, $R_{OH} = (0.95)^{-1}\, R_P$.

The reaction between $^1O_2$ and FFA (rate constant $k_{FFA,1O2} = 1.2\times10^8$ M^{-1} s^{-1}; Wilkinson and Brummer, 1981) is in competition with the thermal deactivation of $^1O_2$ by collision with the solvent molecules ($k_d = 2.5\times10^5$ s^{-1}; Halladja et al., 2007). FFA can also react with $^\bullet$OH, but the rate of

such a reaction is usually negligible compared to FFA + $^1O_2$. The initial degradation rate of FFA can be expressed as follows:

$$R_{FFA} = R_{^1O_2} \frac{k_{FFA,^1O_2} FFA_o}{k_{FFA,^1O_2} FFA_o + k_d} \quad (3)$$

where R_{1O2} is the formation rate of $^1O_2$ upon irradiation of the sample. With FFA_o = 1.8 mM it is $k_{FFA,1O2}$ FFA_o = 2.2×10^5 s^{-1}, which cannot be neglected compared to k_d. The formation rate of $^1O_2$ upon irradiation of the sample can be determined under the conditions of R_{1O2} » R_{OH} and solving equation (3) for R_{1O2}.

The reaction of ^{3}CDOM* with TMP is in competition with the other deactivation processes, which have rate constant k' ≈ 5×10^5 s^{-1} (Canonica and Freiburghaus, 2001). The reaction between TMP and $^\bullet$OH is usually negligible compared to TMP + ^{3}CDOM*, but the same may not be true of the reaction between TMP and $^1O_2$. The latter reaction is in competition with the thermal deactivation of $^1O_2$ following collision with the solvent. Furthermore, the reaction between TMP and ^{3}CDOM* would consume the triplet states and proportionally prevent their reaction with O_2 to give $^1O_2$. Therefore, the degradation rate of TMP due to reaction with $^1O_2$, $R_{TMP}^{^1O_2}$ can be expressed as follows (Minella et al., 2011):

$$R_{TMP}^{^1O_2} = R_{^1O_2} \cdot \frac{k'}{k' + k_{TMP,^3CDOM*} \cdot TMP_o} \cdot \frac{k_{TMP,^1O_2} \cdot TMP_o}{k_d + k_{TMP,^1O_2} \cdot TMP_o} \quad (4)$$

where $k_{TMP,^1O_2}$ = (6.2±1.0)$\times10^7$ M^{-1} s^{-1} (Tratnyek and Hoigné, 1994) and TMP_o = 2.0 mM. The rate $R_{TMP}^{^1O_2}$ contributes to the measured transformation rate of TMP, R_{TMP}, together with the reaction between ^{3}CDOM* and TMP. R_{TMP} can thus be expressed as follows:

$$R_{TMP} = R_{^3CDOM*} \frac{k_{TMP,^3CDOM*} TMP_o}{k_{TMP,^3CDOM*} TMP_o + k'} + R_{TMP}^{^1O_2} \quad (5)$$

where $R_{TMP}^{^1O_2}$ is given by equation (4). In a previous field study, $k_{TMP,^3CDOM*}$ was found to be 3.0×10^9 M^{-1} s^{-1} in Rhône delta lagoons, and the same rate constant value could be applied to both freshwater and brackish samples (Al Housari et al. 2010). Such rate constant compares well with the value of 2×10^9 M^{-1} s^{-1} obtained by Halladja et al. (2007) in the presence of humic acids under irradiation. With $k_{TMP,^3CDOM*}$ = 3.0×10^9 M^{-1} s^{-1} and TMP_o = 2.0 mM, $k_{TMP,^3CDOM*} TMP_o$ = 6.0×10^6

s^{-1}, which does not allow *k'* in equation (5) to be neglected. Therefore, the formation rate of ^{3}CDOM* (R_{3CDOM*}) can be expressed as follows:

$$R_{^3CDOM*} = (R_{TMP} - R_{TMP}^{^1O_2}) \cdot \frac{k_{TMP,^3CDOM*}\, TMP_o + k'}{k_{TMP,^3CDOM*}\, TMP_o} \qquad (6)$$

Equation (6) is valid if $R_{3CDOM*} \gg R_{OH}$, which is usually the case for surface waters (Al Housari et al., 2010).

3. Results

3.1. In situ measurements

Dissolved oxygen concentrations and pH were significantly higher in F1, the sampling site located closest to the tidal sea gate (Table 1). The concentration of dissolved organic carbon (DOC, measured as NPOC) was higher in site F2. Salinity and temperature measurements were similar in both sites. The concentrations of nitrate were below the analytical detection limit (1 µM) in both F1 and F2, while the concentrations of nitrite were around 0.05 µM. Chlorophyll-a related fluorescence was significantly higher in F1 with respect to F2. Chlorophyll-a related fluorescence measurements of filtered water samples showed similar values (2.4 ± 0.4 AU and 2.6 ± 0.2 AU).

3.2. CDOM characteristics

Absorption spectra were broad and unstructured, with the expected near-exponential decrease with increasing wavelength in the ultraviolet and visible wavelengths. The highest absorption was measured in the sample F2 with respect to F1 (Figure 3a).

The distribution of the absorption spectral slope S(λ) was determined between 240 and 600 nm, using 20 nm wavelength intervals. An exponential fitting was found to be appropriate ($p < 0.01$) for the absorption data from 240 to 390 nm for all samples. The resulting spectral slope distribution (Figure 3b) indicated that the difference between the samples is most significant for spectral slopes between 285 nm and 350 nm. Sample F2 had higher spectral slope than F1. In comparison to purely allochthonous and autochthonous CDOM sources, the Fogliano samples had much higher S(λ) values than those determined from the humic-like CDOM from Laguna Iberá (allochthonous CDOM; Galgani et al., 2010) and presented a spectrally variable distribution, with

some analogy to exudates from a laboratory monoculture of the freshwater Chlorophyta *Chlorella* (Loiselle et al. 2009a).

3.3. Optical photodegradation

The change in CDOM absorption was measured in relation to the cumulative dose *D* of solar UV irradiance (Table 2). Solar irradiation of sample F1 induced a clear and significant reduction ($p < 0.05$) of absorption with increasing dose between 240 and 440 nm. The reduction in absorption with exposure was significant between 240 and 365 nm for sample F2. Darkened control samples did not show a significant change in absorption over time. The absolute change in absorption with increasing dose (m^{-1} (kJ m^{-2})$^{-1}$) was used to determine a spectral photodegradation rate. For wavelengths below 400 nm, F1 had a higher photodegradation rate with respect to F2 while both had a significantly lower rate with respect to the humic-like CDOM from Laguna Iberá (Figure 4).

The absorption spectral slope $S(\lambda)$ increased with irradiance dose *D* for most wavelengths below 350 nm and decreased in the wavelengths between 375 nm 390 nm. The rate of change in the absorption spectral slope $S(\lambda)$ with irradiance dose (nm^{-1} (kJ m^{-2} nm^{-1})$^{-1}$) was significantly higher in the F1 sample ($p < 0.05$) between 250 nm and 315 nm, and between 320 and 375 nm (Figure 5). This rate of change was generally higher than that measured in Laguna Iberá.

3.4. Reactive species photoproduction

The photoproduction of phenol from benzene was significantly higher in the F1 sample (Figure 6), $R_P^{F1} = (3.3 \pm 0.1) \times 10^{-11}$ M s^{-1} with respect to $R_P^{F2} = (2.4 \pm 0.4) \times 10^{-11}$ M s^{-1}. The phenol formation rates as a function of the absorbed irradiance dose *D* were $R'_P{}^{F1} = (2.0 \pm 0.1) \times 10^{-8}$ M m^2 kJ^{-1} and $R'_P{}^{F2} = (6.3 \pm 0.1) \times 10^{-9}$ M m^2 kJ^{-1}. The $^{\bullet}OH$ formation rates were $R_{OH}^{F1} = (3.5 \pm 0.1) \times 10^{-11}$ M s^{-1} [corresponding to $(2.1 \pm 0.1) \times 10^{-8}$ M m^2 kJ^{-1}] and $R_{OH}^{F2} = (2.5 \pm 0.4) \times 10^{-11}$ M s^{-1} [$(6.5 \pm 0.1) \times 10^{-9}$ M m^2 kJ^{-1}]. The quantum yields of $^{\bullet}OH$ photoproduction ($\Phi_{OH} = R_{OH} (P_a)^{-1}$) were $\Phi_{OH}^{F1} = (11.1 \pm 0.4) \times 10^{-5}$ and $\Phi_{OH}^{F2} = (3.4 \pm 0.5) \times 10^{-5}$.

The concentrations of nitrate and nitrite, both possible $^{\bullet}OH$ sources in lake water were extremely low (Table 1). Nitrate and nitrite at these low concentrations cannot influence the formation of phenol from 3.0 mM benzene (Vione et al., 2006). Therefore, the vast majority of $^{\bullet}OH$

photo-production in the studied samples would be accounted for by CDOM (Mopper and Zhou, 1990; Vione et al., 2006; Page et al., 2011).

The transformation rate of FFA was lower for F1, $R_{FFA}^{F1} = (4.3 \pm 0.3) \times 10^{-9}$ M s^{-1} with respect to $R_{FFA}^{F2} = (5.1 \pm 0.1) \times 10^{-9}$ M s^{-1} assuming a linear decay (Figure 7). However, the transformation rate per irradiance dose was significantly higher in F1, $R_{FFA}^{F1} = (2.6 \pm 0.2) \times 10^{-6}$ M m^2 kJ^{-1} with respect to $R_{FFA}^{F2} = (1.3 \pm 0.1) \times 10^{-6}$ M m^2 kJ^{-1}. To check for the participation of $^1O_2$ in the transformation of FFA, samples containing 30 mM NaN_3 in addition to 1.8 mM FFA were irradiated, as the azide anion (N_3^-) is an effective scavenger of $^1O_2$ (second-order rate constant 1.7×10^9 M^{-1} s^{-1} at pH 8.4; Wilkinson and Brummer, 1981). The azide-added samples showed negligible transformation of FFA at the adopted irradiation time scale (Figure 7), suggesting that $^1O_2$ was the main reactive species involved in the FFA degradation. The resulting formation rates of singlet oxygen were determined to be $R_{1O2}^{F1} = (9.2 \pm 0.7) \times 10^{-9}$ M s^{-1} [$(5.6 \pm 0.4) \times 10^{-6}$ M m^2 kJ^{-1}] and $R_{1O2}^{F2} = (1.1 \pm 0.2) \times 10^{-8}$ M s^{-1} [$(2.9 \pm 0.5) \times 10^{-6}$ M m^2 kJ^{-1}]. In both cases, it is $R_{1O2} \gg R_{OH}$, which confirms the applicability of equation (3). The quantum yields for $^1O_2$ photo-production are $\Phi_{1O2}^{F1} = (2.9 \pm 0.2) \times 10^{-2}$ and $\Phi_{1O2}^{F2} = (1.5 \pm 0.3) \times 10^{-2}$. The latter yield is similar to that reported for numerous lakes in northern Italy (Vione et al., 2010a). Considering that irradiated CDOM would be the only important source of $^1O_2$ in surface waters (Hoigné, 1990; Al Housari et al., 2010), it can be inferred that CDOM in sample F1 would produce $^1O_2$ more effectively than CDOM in F2 for the same irradiance dose ($\Phi_{1O2}^{F1} > \Phi_{1O2}^{F2}$).

The degradation of TMP showed significant differences between the two samples (Figure 8), with $R_{TMP}^{F1} = (8.0 \pm 0.7) \times 10^{-9}$ M s^{-1} [$(4.9 \pm 0.4) \times 10^{-6}$ M m^2 kJ^{-1}] and $R_{TMP}^{F2} = (1.5 \pm 0.1) \times 10^{-8}$ M s^{-1} [$(3.9 \pm 0.3) \times 10^{-6}$ M m^2 kJ^{-1}]. The formation rates of ^{3}CDOM* were $R_{3CDOM*}^{F1} = (8.4 \pm 0.7) \times 10^{-9}$ M s^{-1} [$(5.3 \pm 0.4) \times 10^{-6}$ M m^2 kJ^{-1}] and $R_{3CDOM*}^{F2} = (1.6 \pm 0.1) \times 10^{-8}$ M s^{-1} [$(4.2 \pm 0.3) \times 10^{-6}$ M m^2 kJ^{-1}], obtained from equation (5) that is applicable because $R_{3CDOM*} \gg R_{OH}$. The multi-wavelength quantum yields (Φ_{3CDOM*}) were $(2.7 \pm 0.2) \times 10^{-2}$ and $(2.2 \pm 0.1) \times 10^{-2}$ for F1 and F2, respectively.

4. Discussion

The spectral photodegradation rates and the quantum yields of transient photoproduction showed clear differences between samples, with F1 being more photo-reactive even though it had the lowest CDOM absorption and DOC concentration (see also Wenk et al., 2011; Guerard et al., 2009). Both samples showed the largest absorption loss below 300 nm, where incident solar irradiance is minimal. In comparison, both samples showed a smaller photodegradation rate compared to the humic-like CDOM from Laguna Iberá (Galgani et al., 2010).

The rate of change of S(λ) indicated that F1 underwent a larger modification (decrease) in average molecular weight (MW) for the same irradiance dose with respect to F2, considering that larger S(λ) values are usually associated with CDOM molecules having smaller average MW (Peuravuori and Pihlaja, 1997; Blough and Del Vecchio, 2002; Helms et al., 2008). In comparison to the humic-like CDOM of Laguna Iberá, the S(λ) rates of change for the two samples from Fogliano Lake were higher in absolute values, especially between 240 nm and 280 nm. This indicates that, while the overall photodegradation rate (loss of absorption) of the Fogliano Lake samples was inferior to that of Laguna Iberá, the relative change in molecular weight (or humic/fulvic ratio) was higher in Fogliano Lake (F1 in particular) with increased irradiance dose.

The photoproduction quantum yields for $^{\bullet}OH$ (Φ_{OH}), $^1O_2$ (Φ_{1O2}) and ^{3}CDOM* (Φ_{3CDOM*}) were consistently higher for F1 with respect to F2. It should be noted that $\Phi_{3CDOM*}^{F1} \sim \Phi_{1O2}^{F1}$ and that $^1O_2$ is generated by the reaction between ^{3}CDOM* and ground-state O_2 (Hoigné et al., 1990). Therefore, it would appear that practically all the triplet states of F1 were able to produce $^1O_2$. On the other hand, $\Phi^{F2}_{3CDOM*} > \Phi^{F2}_{1O2}$, meaning that a significant fraction (some 30 ± 10 %) of the excited triplet states of the F2 sample did not react with ground-state oxygen to produce $^1O_2$. This is not surprising if one considers that the triplet state of anthraquinone-2-sulphonate does not yield $^1O_2$ (Maddigapu et al., 2010), and that quinones are important components of CDOM (Cory and McKnight, 2005). Nevertheless, this finding further confirms that the CDOM at the two sites was significantly different.

Previous studies have shown that photogenerated transients react with CDOM and can contribute to a loss in absorption (Scully et al., 2003). A main difficulty to relating photodegradation to transient formation rates is the poor characterization of both transient species (in particular ^{3}CDOM*) as well as the CDOM itself. However, it is possible to identify which of the

transient species are most likely to contribute to photodegradation by comparing transient formation rates and photodegradation rates with the following assumptions: *(i)* non-chromophoric DOM and CDOM react at comparable rates and on an equimolar basis with photogenerated transients (*e.g.* ^{3}CDOM* or $^\bullet$OH), and *(ii)* such a reaction reduces CDOM absorbance. Considering that the decrease of absorbance (*e.g.* at 270 nm) is likely to follow pseudo-first order kinetics, as in similar photochemical reactions (Vione et al., 2009b), one obtains:

$$A = A_o \cdot e^{-k \cdot D} \qquad (7)$$

where ***D*** is the cumulative absorbed dose and k is the dose-related rate constant. For limited exposure as in the present case, a pseudo-first order decay of absorbance would not differ significantly from a linear trend. The relative rate constants would be $k_{F1} = 8 \times 10^{-3}$ m^2 kJ^{-1} and $k_{F2} = 3 \times 10^{-3}$ m^2 kJ^{-1}. The DOM concentration, derived from NPOC values, is $C_{F1} = 2.2 \times 10^{-4}$ mol C L^{-1} and $C_{F2} = 2.6 \times 10^{-4}$ mol C L^{-1}. If the decrease in absorbance was caused by a reaction between CDOM and transients and if DOM and CDOM reacted at comparable rates with the transients, the reaction rates between DOM and transients would be: $R_{F1} = k_{F1}\ C_{F1} = 2 \times 10^{-6}$ mol C L^{-1} m^2 kJ^{-1} and $R_{F2} = 8 \times 10^{-7}$ mol C L^{-1} m^2 kJ^{-1}.

For ^{3}CDOM* as reactive transient, the reaction with DOM/CDOM would be in competition with other quenching processes (thermal deactivation, reaction with O_2). Using a steady-state approximation for ^{3}CDOM*, the rate of reaction can be expressed as follows:

$$R_8 = R_{^3CDOM^*} \cdot \frac{k_8 \cdot C_{DOM}}{k_8 \cdot C_{DOM} + k'} \qquad (8)$$

where C_{DOM} is the concentration of organic carbon in units of mol C L^{-1}, k_8 is the second-order rate constant between DOM/CDOM and ^{3}CDOM*, and the rate constant of other quenching processes of ^{3}CDOM* is $k' \approx 5 \times 10^5$ s^{-1} (Canonica and Freiburghaus, 2001). By examining the ratios of $R_8^{F1}\ R_{F1}^{-1}$ and $R_8^{F2}\ R_{F2}^{-1}$ as a function of k_8 (Figure 9), it is possible to show that ^{3}CDOM* could contribute significantly to photodegradation rates for $k_8 > 5 \times 10^7$ L (mol C)$^{-1}$ s^{-1}. This is within the range of values obtained between triplet aromatic ketones (used as ^{3}CDOM* proxies) and phenylurea herbicides, 10^6 - 10^8 L (mol C)$^{-1}$ s^{-1} (Canonica et al., 2006). The range of k_8 values in Figure 9 ensures that $k_8\ C_{DOM} < k'$, which is reasonable for surface waters (Canonica and Freiburghaus, 2001).

Reactive triplet states are usually oxidizing agents, thus they would often react with ground-state organic molecules by electron or hydrogen abstraction. Multiple oxidative steps can for instance break conjugation or cleave aromatic rings, while formation of new rings is usually less common. In contrast, species formed by triplet reduction would often react with dissolved O_2 to give back the initial compound (Maurino et al., 2011).

The contribution of $^1O_2$ might also be significant as formation rates R_{1O2} are similar to R_{3CDOM*} and the deactivation rate constants of the two species in aqueous solution are of the same order of magnitude. However, $^1O_2$ is often less reactive than ^{3}CDOM* (Halladja et al., 2007).

On the other hand, $^{\bullet}$OH would not play an important role in the loss of absorption in the present samples, as $R_{OH}^{F1} \ll R_{F1}$ and $R_{OH}^{F2} \ll R_{F2}$, with differences of about two orders of magnitude. Earlier studies have shown that $^{\bullet}$OH plays a minor role in DOM photomineralization (Brinkmann et al., 2003; Vione et al., 2009a). Here we show that it should not play a significant role in the decrease in CDOM absorption. Note that negligible DOM mineralization was observed in the irradiated samples (NPOC values were practically constant during lake-water irradiation, data not shown), thus significant absorption loss was not accompanied by an equivalent loss of organic carbon. The lack of mineralization would be consistent with the limited role of $^{\bullet}$OH in the studied processes, as the hydroxyl radical is usually involved in pathways that finally lead to the mineralization of organic compounds (Iurascu et al., 2009).

An additional issue is that the direct photolysis processes of organic molecules often proceed through the transformation of their triplet states (Boule et al., 2005; Vione et al., 2010b). Thus, it is interesting to compare the values of R_{F1} and R_{F2} (respectively, 2×10^{-6} mol C L^{-1} m^2 kJ^{-1} and 8×10^{-7} mol C L^{-1} m^2 kJ^{-1}) with R_{3CDOM*}^{F1} and R_{3CDOM*}^{F2} (respectively, $(5.3 \pm 0.4) \times 10^{-6}$ M m^2 kJ^{-1} and $(4.2 \pm 0.3) \times 10^{-6}$ M m^2 kJ^{-1}). Note that organic compounds of CDOM contain several C atoms, thus the R_{3CDOM*} values in mol C L^{-1} units (instead of triplet state molarity M) would be higher. As $R_{3CDOM*}^{F1} > R_{F1}$ and $R_{3CDOM*}^{F2} > R_{F2}$, there is the potential that direct photolysis processes that proceed through triplet-state formation are involved in the loss of absorption. Such processes would not occur with high efficiency as energy dissipation reactions would compete with ^{3}CDOM* transformation. For F1, a major issue would be the very efficient reaction between ^{3}CDOM* and O_2 to give $^1O_2$, an energy-transfer process that would usually give back the unmodified, ground-state CDOM (Boule et al., 2005).

5. Conclusions

In the present study, CDOM samples from a small shallow lake showed markedly different sensitivities to solar radiation. Such differences are likely associated to a variation in CDOM sources or sinks. While, similar CDOM sources were present throughout the lake, the F2 site is characterized by a higher summertime density of submersed macrophytes while F1 had a higher phytoplankton biomass during the measurement period. Regarding CDOM sinks, UV attenuation was higher in F2, where autoshading by CDOM limits the penetration of UV within the water column. Dilution effects on CDOM can be assumed to be significantly higher in F1, located much closer to the sea gate and therefore more sensitive to tidal currents. However, the significantly different $S(\lambda)$ as well as the transient species quantum yields indicate that dilution alone does not control CDOM dynamics.

These moderately different conditions led to a significant difference in photodegradation and transient formation rates. The CDOM present in F2, with a higher absorption and higher DOC concentration was found to be significantly less photoreactive and had lower quantum yields of transient formation than the F1 sample. This reduced photoreactivity is likely to be associated to residence time, as the higher $S(\lambda)$ of the F2 sample (suggesting lower average MW) would indicate a longer history of exposure. It is likely that F2 is characterized by more recalcitrant CDOM which accumulated in this part of the lake.

In both sites, indirect photodegradation processes (*sensu* Del Vecchio and Blough, 2004) were important in modifying the CDOM optical properties. The spectral distribution of photodegradation had the highest rates below 300 nm, where exposure to solar radiation was very limited (due to the lack of solar irradiance in these wavelengths as well as the screening effect of the Tedlar). Changes in absorption were consistent with the photochemical production of transient species, most notably ^{3}CDOM* and possibly $^1O_2$. In contrast, $^\bullet$OH was unlikely to play a significant role. The triplets ^{3}CDOM* play an important role in absorption changes, either via their direct chemical modification or upon reaction with ground-state CDOM, as their formation rates were high enough to account for changes in absorption. These processes could explain the observed connection between absorbance decrease and the quantum yield of transient (^{3}CDOM*) photoproduction.

The present study shows that the production of reactive species by CDOM plays a significant role in CDOM photodegradation in the shallow waters of Fogliano Lake. This represents a first step in combining optical and transient species analysis to better understand CDOM photodegradation processes in the natural environment.

Acknowledgements

This work was supported by the Circle-Med initiative (http://www.circle-med.net/) on climate change impacts in the Mediterranean region. The Italian Interuniversity Consortium CSGI, the National Park of Circeo and the Italian Ministry for Agricultural and Forest Policies also supported this research.

References

Al Housari, F., Vione, D., Chiron S., Barbati S., 2010. Reactive photoinduced species in estuarine waters. Characterization of hydroxyl radical, singlet oxygen and dissolved organic matter triplet state in natural oxidation processes. Photochem. Photobiol. Sci. 9, 78-86.

Albinet, A., Minero C., Vione D., 2010. Phototransformation processes of 2,4-dinitrophenol, relevant to atmospheric water droplets. Chemosphere 80, 753-758.

Blough, N. V., Del Vecchio R. 2002. Distribution and dynamics of chromophoric dissolved organic matter (CDOM) in the coastal environment, In : Biogeochemistry of marine dissolved organic matter (Hansell, D. and Carlson, C., Eds.). Academic Press. pp. 509–546.

Boreen, A. L., Edhlund, B. L., Cotner, J. B., McNeill, K., 2008. Indirect photodegradation of dissolved free amino acids: The contribution of singlet oxygen and the differential reactivity of DOM from various sources. Environ. Sci. Technol. 42, 5492-5498.

Boule, P., Bahnemann D. W., Robertson P. K. J., 2005. The Handbook of Environmental Chemistry. Vol. 2.M (Environmental Photochemistry Part II), Springer, Berlin.

Bracchini L., Dattilo, A. M., Falcucci, M., Hull, V., Tognazzi, A., Rossi, C., Loiselle, S. A., 2011. Competition for spectral irradiance between epilimnetic optically active dissolved and suspended matter and phytoplankton in the metalimnion. Consequences for limnology and chemistry. Photochem. Photobiol. Sci. doi:org/10.1039/C0PP00291G

Bracchini L., Dattilo, A.M., Falcucci, M., Loiselle, S.A., Hull, V., Arena, C. and Rossi, C., 2005. Spatial and temporal variations of the inherent and apparent optical properties in a shallow coastal lake. J. Photoch. Photobio. B 80, 161-177.

Brinkmann, T., Hörsch, P., Sartorius, D., Frimmel, F. H., 2003. Photoformation of low-molecular-weight organic acids from brown water dissolved organic matter. Environ. Sci. Technol. 37, 4190-4198.

Buxton, G. V., Greenstock, C. L., Helman, W. P., Ross, A. B., 1988. Critical review of rate constants for reactions of hydrated electrons, hydrogen atoms and hydroxyl radicals ($^{\bullet}OH/^{\bullet}O^{-}$) in aqueous solution. J. Phys. Chem. Ref. Data 17, 1027-1284.

Canonica, S., Freiburghaus M., 2001. Electron-rich phenols for probing the photochemical reactivity of freshwaters. Environ. Sci. Technol. 35, 690-695.

Canonica, S., Hellrung, B., Muller, P., Wirz, J., 2006. Aqueous oxidation of phenylurea herbicides by triplet aromatic ketones. Environ. Sci. Technol. 40, 6636-6641.

Chen, Z. Hu, C., Conmy, R. N., Muller-Karger, F., Swarzenski, P. 2007. Colored dissolved organic matter in Tampa Bay, Florida. Mar. Chem. 104, 98-109.

Cory, R. M., McKnight D. M., 2005. Fluorescence spectroscopy reveals ubiquitous presence of oxidized and reduced quinones in dissolved organic matter. Environ. Sci. Techol. 39, 8142-8149.

Del Vecchio, R., Blough N.V., 2004. On the origin of the optical properties of humic substances. Environ. Sci. Techol. 38, 3885-3891.

Guerard, J. J.; Miller, P:L, Trouts, T., Chin, YP., 2009. The role of fulvic acid composition in the photosensitized degradation of aquatic contaminants. Aquatic Sciences 71:160-169

Galgani L., Tognazzi, A., Rossi, C., Ricci, M., Galvez, J. A., Dattilo, A. M., Cozar, A. Bracchini, L., Loiselle, S.A., 2011. Assessing the optical changes in dissolved organic matter in humic lakes by spectral slope distributions. J. Photoch. Photobio. B. 102, 132-139.

Halladja, S., Ter Halle, A., Aguer, J. P., Boulkamh, A., Richard, C., 2007. Inhibition of humic substances mediates photooxigenation of furfuryl alcohol by 2,4,6-trimethylphenol. Evidence for reactivity of the phenol with humic triplet excited states. Environ. Sci. Technol. 41, 6066-6073.

Helms, J.R., Stubbins, A., Ritchie, J.D., Minor, E., Kieber, D.J., Mopper K., 2008. Absorption spectral slopes and slope ratio as indicators of molecular weight, source and photobleaching of chromophoric dissolved organic matter. Limnol. Oceanog. 53, 955-9609.

Hoigné, J., 1990. Formulation and calibration of environmental reaction kinetics: Oxidations by aqueous photooxidants as an example. In: Aquatic Chemical Kinetics, Stumm, W. (Ed.), Wiley, NY, pp. 43-70.

Kieber, R. J., Seaton, P. J., 1996. Determination of subnanomolar concentrations of nitrite in natural waters. Anal. Chem. 67, 3261-3264.

Kuhn, H. J., Braslavsky, S. E., Schmidt, R., 2004. Chemical actinometry. Pure Appl. Chem. 76, 2105-2146.

Iurascu, B., Siminiceanu, I., Vione, D., Vicente, M. A., Gil, A., 2009. Phenol degradation in water through a heterogeneous photo-Fenton process catalyzed by Fe-treated laponite. Wat. Res. 43, 1313-1322.

Loiselle, S. A., Bracchini, L., Dattilo, A. M., Ricci, M., Tognazzi, A., Cozar, A., Rossi, C., 2009a. The optical characterization of chromophoric dissolved organic matter using the wavelength distribution of absorption spectral slopes. Limnol. Oceanog. 54, 590-597.

Loiselle, S. A., Bracchini, L., Cózar, A., Dattilo, A. M., Tognazzi, A., Rossi, C., 2009b. Variability in photobleaching rates and their related impacts on optical conditions in subtropical lakes. J. Photoch. Photobio. B. 95, 129-137.

Maddigapu, P.R., Bedini, A., Minero, C., Maurino, V., Vione, D., Brigante, M., Mailhot, G. and Sarakha, M., 2010. The pH-dependent photochemistry of anthraquinone-2-sulphonate. Photochem. Photobiol. Sci. 9, 323-330.

Maurino, V., Bedini, A., Borghesi, D., Vione, D., Minero, C., 2011. Phenol transformation photosensitised by quinoid compounds. Phys. Chem. Chem. Phys. 13, 11213-11221.

Minella, M., Romeo, F., Vione, D., Maurino, V., Minero, C., 2011. Low to negligible photoactivity of lake-water matter in the size range from 0.1 to 5 µm. Chemosphere 83, 1480-1485.

Mopper, K., Zhou X., 1990. Hydroxyl radical photoproduction in the sea and its potential impact on marine processes. Science 250, 661-664.

Moran, M. A., Sheldeon, W. M., Zepp R. G., 2000. Carbon loss and optical property changes during long term photochemical, biological degradation of estuarine dissolved organic matter. Limnol. Oceanogr. 45, 1254–1264.

Page, S. E., Arnold, W. A., McNeill K., 2011. Assessing the contribution of free hydroxyl radical in organic-matter sensitized photohydroxylation reactions. Environ. Sci. Technol. 45, 2818-2825.

Peuravuori, J., Pihlaja, K., 1997. Molecular size distribution and spectroscopic properties of aquatic humic substances. Anal. Chim. Acta 337, 133-149.

Scully, N. M., Cooper, W. J., Tranvik, L. J., 2003. Photochemical effects on microbial activity in natural waters: the interaction of reactive oxygen species and dissolved organic matter. FEMS Microb. Ecol. 46, 353-357.

Signorini, A., Massini, G., Migliore, G., Tosoni, M., Marrone, C., Izzo, G., 2008. Sediment biogeochemical differences in two pristine Mediterranean coastal lagoons (in Italy) characterized by different phanerogam dominance - A comparative approach. Aquat. Conserv. 18, S27-S44.

Sulzberger, S., Durisch-Kaiser E., 2009. Chemical Characterization of dissolved organic matter (DOM): A prerequistite for underestanding UV-induced changes of DOM absorption properties and bioavailability. Aquat. Sci. 71; 104-126.

Takeda, K., Takedoi, H., Yamaji, S., Ohta, K., Sakugawa, H., 2004. Determination of hydroxyl radical photoproduction rates in natural waters. Anal. Sci. 20, 153-158.

Talling, J.F., Driver D., 1963. Some problems in the estimation of chlorophyll-a in phytoplankton. In: Proc. Conference of Productivity Measurements. Marine and Freshwaters. pp. 142–146. University of Hawaii, Hawaii.

Tranvik, L.J., Downing, J.A., Striegl, R.G., Cotner, J.B., Loiselle, S.A., Renwick, W.H., Roland, F., Kutser, T., Finlay, K., Sobeck, S., McCallister, L.S., Melack, J.M., Kortelainen, P.L., Leech, D.M., Weyhenmeye, G.H., Porter, J.A., Tremblay, A., Dillon, P., Laurion, I., vonWachenfeldt, E., McKnight, D.M., Verschoor, A., Ballatorem, T.J., Larsen, S., Sherman, B.S., Overholt, E., Vanni, M.J., Knoll, L.B., Fortino, K., Schindler, D.W. ,Prairie. Y., 2009. Lakes and impoundments as regulators of carbon cycling and climate. Limnol. Oceanog. 54, 2298–2314.

Tratnyek, P. G. Hoigné, J., 1994. Photo-oxidation of 2,4,6-trimethylphenol in aqueous laboratory solutions and natural waters: Kinetics of reaction with singlet oxygen. J. Photoch. Photobio. A. 84, 153-160.

Vione, D., Falletti, G., Maurino, V., Minero, C., Pelizzetti, E., Malandrino, M., Ajassa, R., Olariu, R.I., Arsene, C., 2006. Sources and sinks of hydroxyl radicals upon irradiation of natural water samples. Environ. Sci. Technol. 40, 3775-3781.

Vione, D., Lauri V., Minero C., Maurino V., Malandrino M., Carlotti M.E., Olariu R.I., Arsene C., 2009a. Photostability and photolability of dissolved organic matter upon irradiation of natural water samples under simulated sunlight. Aquat. Sci. 71, 34-45.

Vione, D., Minella, M., Minero, C., Maurino, V., Picco, P., Marchetto, A., Tartari, G., 2009b. Photodegradation of nitrite in lake waters: Role of dissolved organic matter. Environ. Chem. 6, 407-415.

Vione, D., Rinaldi, E., Minero, C., Maurino, V., Olariu, R.-I., Arsene, C., 2009c. Studies regarding groundwater quality at rural sites. 2. Photochemical generation of $^{\bullet}OH$ and $^{\bullet}NO_2$ radicals upon UV-A irradiation of nitrate-rich groundwater. Rev. Chim. 60, 551-554.

Vione, D., Bagnus, D., Maurino, V., Minero C., 2010a. Quantification of singlet oxygen and hydroxyl radicals upon UV irradiation of surface water. Environ. Chem. Lett. 8, 193-198.

Vione, D., Khanra, S., Das, R., Minero, C., Maurino, V., Brigante, M., Maihlot, G., 2010b. Effect of dissolved organic compounds on the photodegradation of the herbicide MCPA in aqueous solution. Wat. Res. 44, 6053-6062.

Wenk, J., Von Gunten U., Canonica S., 2011. Effect of dissolved organic matter on the transformation of contaminants induced by excited triplet states and the hydroxyl radical. Environ. Sci. Technol. 45, 1334-1340.

Wilkinson, F., Brummer J., 1981. Rate constants for the decay and reactions of the lowest electronically excited singlet-state of molecular oxygen in solution. J. Phys. Chem. Ref. Data 10, 809-1000.

Zhang,Y. van Dijk, M. A., Liu, M., Zhu, G., Qin, B., 2009. The contribution of phytoplankton degradation to chromophoric dissolved organic matter (CDOM) in eutrophic shallow lakes: Field and experimental evidence. Water Res. 43, 4685-4697.

Table 1. Physical and chemical characteristics of two sampling sites in Fogliano Lake

	Sampling site F1	Sampling site F2
Temperature (±0.1) °C	22.4 °C	23.2°C
pH (±0.1)	8.8	8.6
Salinity (±0.1) PSU	32.8	32.1
Dissolved oxygen (±0.1) mg L-1	6.6	5.3
Nitrate (±1) µM	<1	<1
Nitrite (±0.01) µM	0.05	0.05
Chlorophyll-a fluorescence (±1) AU	55	15
Turbidity (±0.2) NTU	2.6	3.4
NPOC (±0.05) mg C L−1	2.59	3.14

Table 2. Cumulative absorbed (UV) irradiance dose for *in situ* photodegradation experiments at different measurement times (t)

	t1 (±0.1) (kJ/m^2)	t2 (±0.1) (kJ/m^2)	t3 (±0.1) (kJ/m^2)	t4 (±0.1) (kJ/m^2)	t5 (±0.1) (kJ/m^2)
Sample F1	3.8	7.7	8.9	11.4	13.3
Sample F2	4.8	9.7	11.2	14.3	16.7

Figure 1. Sampling sites in Fogliano Lake.

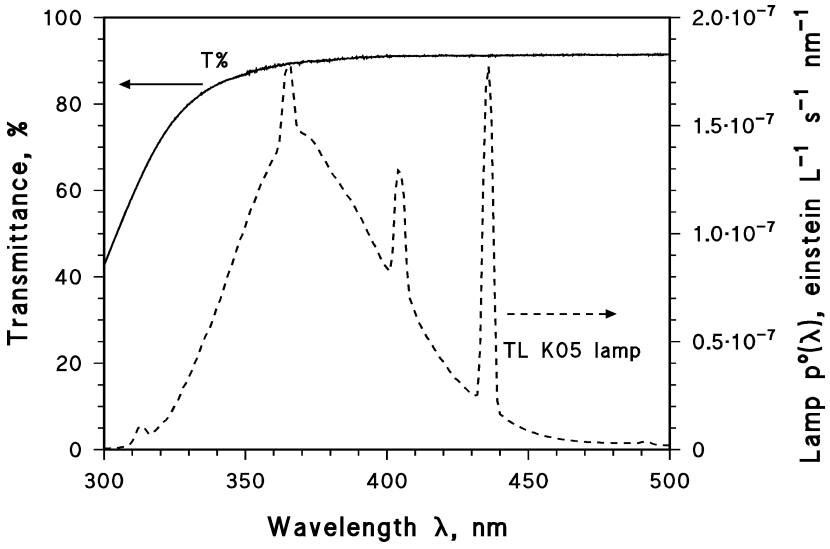

a)

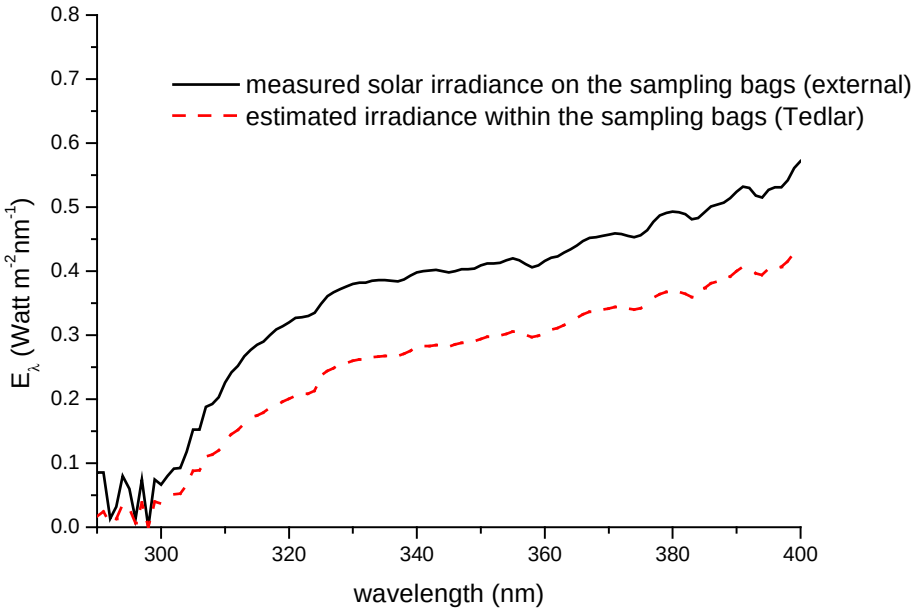

b)

Figure 2. Spectral irradiance on the CDOM samples, a) emission spectrum of the UVA lamps used in the reactivity experiments, transmittance spectrum of the Pyrex glass window of the irradiation cells; b) spectral irradiance on the sample bags and within the sample bags for the photodegradation experiments.

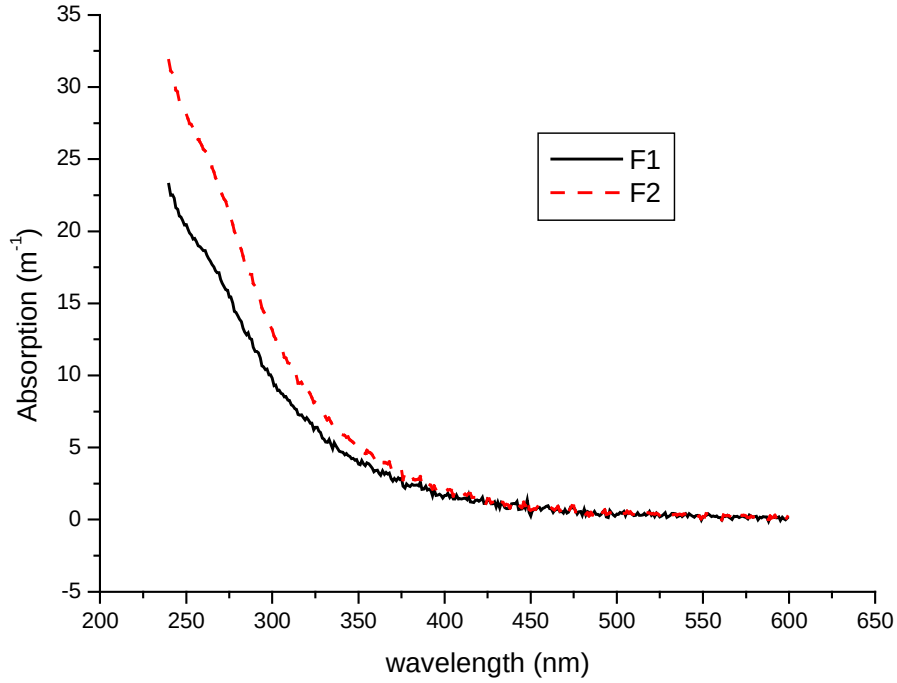

a)

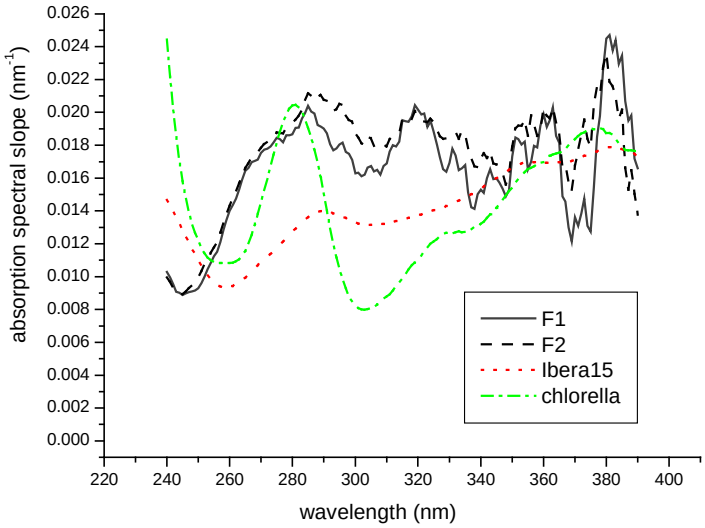

b)

Figure 3. a) CDOM absorption of samples F1 and F2; b) absorption spectral slope distributions (S(λ)) for samples F1 and F2 from Fogliano Lake, Laguna Iberá and exudates from *Chlorella* sample.

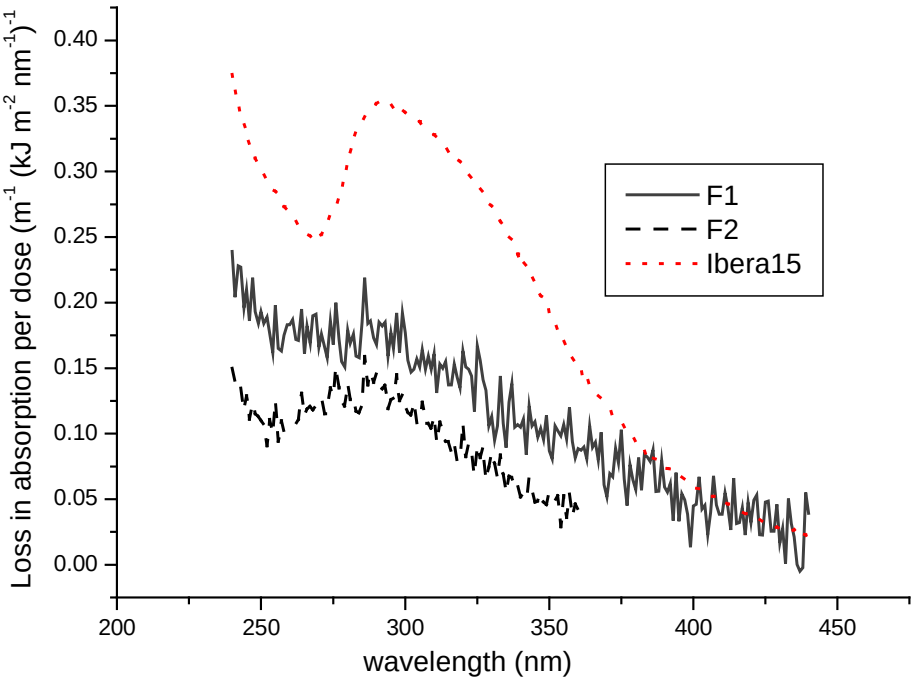

Figure 4. Spectral distribution of the photodegradation rate (loss of absorption with dose ***D***) for CDOM samples from Fogliano Lake and from Laguna Iberá.

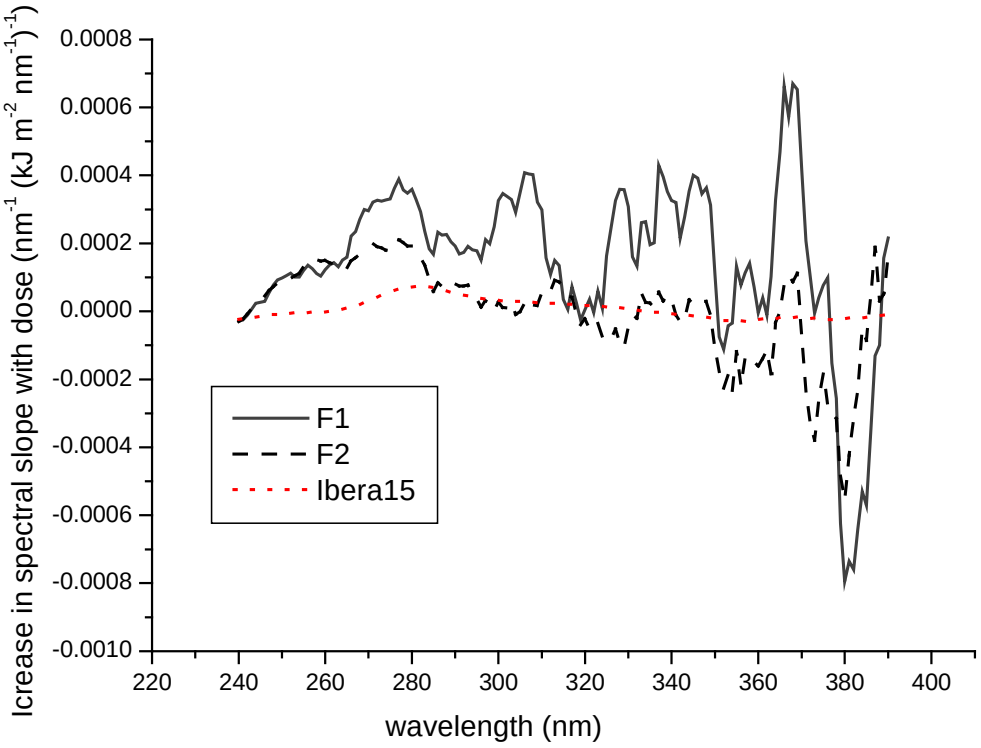

Figure 5. Spectral distribution of the rate of change of S(λ) per unit dose *D* for CDOM samples from Fogliano Lake and from Laguna Iberá.

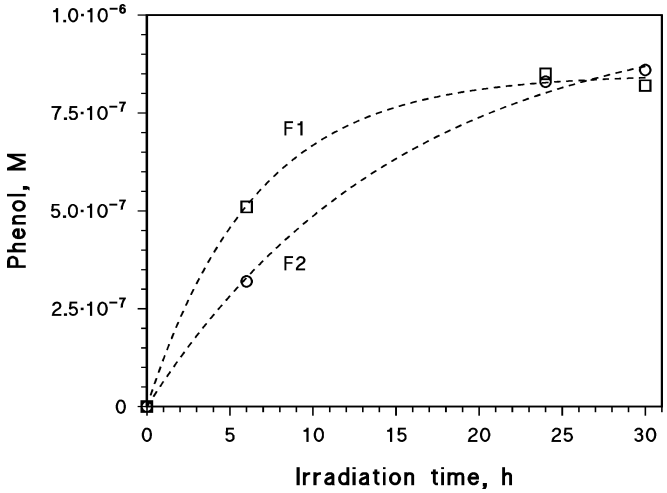

Figure 6. Phenol formation with increasing irradiation time for samples F1 and F2, spiked with benzene to obtain B_o = 3.0 mM.

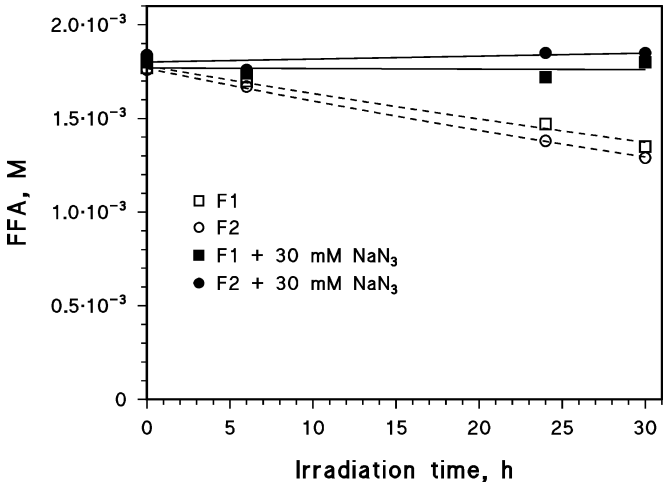

Figure 7. Transformation of FFA (FFA_o = 1.8 mM) in the lake water samples with increasing irradiation time.

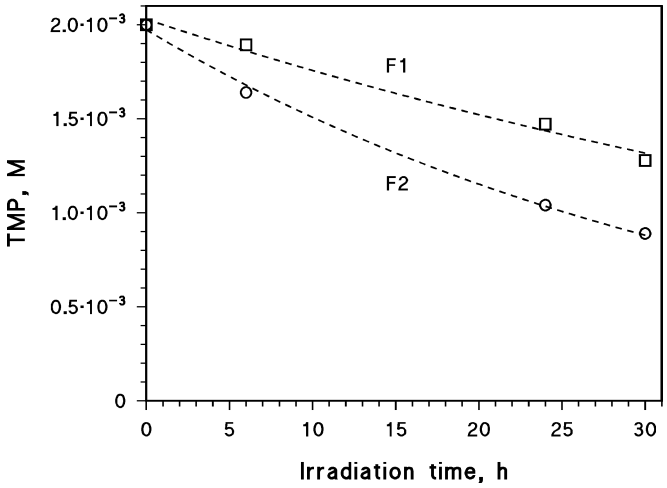

Figure 8. Degradation of TMP (TMP_o = 2.0 mM) in the lake water samples with increasing irradiation time.

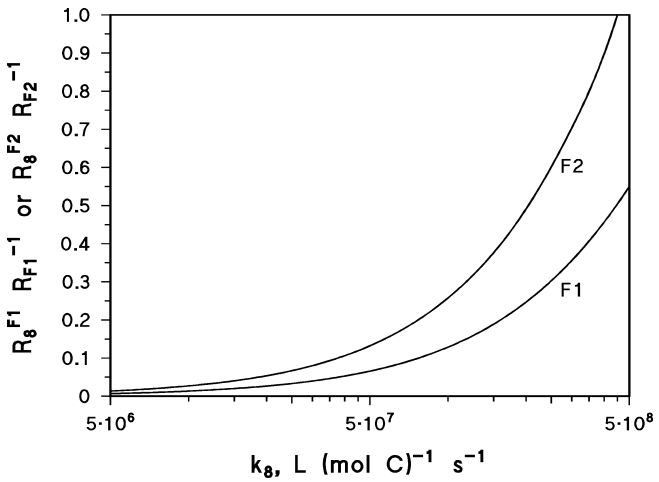

Figure 9. The relative ^{3}CDOM* contribution to CDOM photodegradation, as a function of the rate constant k_8 between ^{3}CDOM* and (C)DOM. Note the logarithmic scale in the X axis.